



A Comparative Analysis of Production Forecast for Vertical Gas Wells: Fractured vs. Non-Fractured

Ekrem Alagoz^{1*}, Emre Can Dundar¹

¹Turkish Petroleum Corporation (TPAO), Ankara, Turkey

INFORMATION

Article history

Received 16 July 2024

Revised 02 August 2024

Accepted 06 August 2024

Keywords

Vertical gas wells

Production forecast

Fractured wells

Darcy flow

Tubing head pressure

Contact

*Ekrem Alagoz

ealagoz@tpao.gov.tr

ABSTRACT

This study delves into the forecasting of gas production from vertical wells, specifically comparing the outcomes between non-fractured and fractured vertical gas wells. Focusing on dry gas extraction from natural gas formations post-transient flow, the analysis adopts assumptions of Darcy flow and zero skin factor. With a constant tubing head pressure as a parameter, the research scrutinizes the production forecasts of both fractured and non-fractured wells, shedding light on the implications of fracture stimulation on gas extraction efficiency and productivity.

1. Introduction

The efficient extraction of hydrocarbons from natural gas formations hinges on accurate production forecasting and a profound understanding of pressure dynamics within gas wells. In this context, the present study addresses the intricate interplay between transient flow behavior and pressure drop phenomena to facilitate optimized gas production strategies.

Gas production forecasting is a critical endeavor, particularly in the context of declining reservoir pressure. With reservoirs experiencing natural depletion over time, it becomes imperative to develop robust forecasts to guide production operations effectively.

As outlined by Smith et al. (2019), accurate forecasting aids in strategic decision-making, resource allocation, and long-term planning in the oil and gas industry.

Additionally, the analysis of pressure drops along the wellbore provides crucial insights into the efficiency and

performance of gas extraction operations. Understanding the components contributing to pressure drop, including friction, acceleration, and gravitational potential, is pivotal in optimizing production processes. This aligns with the findings of Jones and Wang (2020), who emphasize the importance of pressure drop analysis in enhancing well productivity and overall reservoir performance.

Moreover, the influence of well design and completion techniques on production forecasting and pressure dynamics cannot be overlooked. Studies by Lee and Smith (2018) and Chen (2021) have demonstrated the significant impact of well geometry, completion methods, and reservoir characteristics on gas well performance and pressure behavior. There is also detailed research of the mathematical modelling a hydrocarbon shale reservoir with the natural fractures, and its impacts on the well completion and stimulation processes—specifically hydraulic fracturing processes—are analyzed by Dundar et al. (2019), and the study is applied for five most important US shale reservoirs (Dundar et al., 2019).



In-depth research has delved into the dynamics of pressure distribution within pore throats, with a focus on elucidating the fundamental mechanisms governing fluid flow in porous media. Alagoz and Giozza (2023) conducted a sensitivity analysis on bottomhole pressure calculations in two-phase wells, providing valuable insights into the factors influencing pressure dynamics within such systems (Alagoz and Giozza, 2023). Furthermore, Alagoz et al. (2023) have contributed to the field by developing computational tools for analyzing wellbore stability, thereby enhancing our understanding of pressure behavior in complex geological formations (Alagoz et al., 2023). These studies have laid the groundwork for comprehending pressure dynamics in pore throats and have paved the way for further exploration in this area.

In the introduction page, the foundational works in the field provide essential context for this comparative study. Prior research has extensively explored various aspects of gas production forecasting, focusing on factors such as reservoir characteristics, well configurations, and operational parameters. Notably, studies have investigated the impact of Darcy flow and zero skin factor assumptions on production forecasts in non-fractured vertical gas wells. Additionally, research has delved into the effectiveness of fracture stimulation techniques in enhancing gas recovery rates from fractured wells under different reservoir conditions. Building upon this existing body of knowledge, our study aims to contribute valuable insights by directly comparing the production forecasts of non-fractured and fractured vertical gas wells, with a specific emphasis on the influence of fracture stimulation on gas extraction efficiency. Through rigorous analysis and interpretation of results, this research endeavors to advance understanding in the field and inform decision-making processes in gas production operations.

2. Related Works

In the topic of production forecasting, significant studies have been made in assessing various empirical and advanced modeling techniques to improve prediction accuracy. One such study by Laalam et al. (2024) comprehensively compared 11 empirical decline curve models with modern time series models, including ARIMA, LSTM, and GRUs, for predicting production in unconventional oil wells in the Wolfcamp Formation, Midland Basin. The findings showed that no single model consistently excelled across all wells, necessitating customized approaches for each well to optimize forecasting accuracy. These findings underscore the potential of advanced machine learning and time series analysis to provide more precise and reliable forecasts, contributing to better decision-making and optimized field development strategies in the oil and gas industry.

Similarly, another study by Laalam et al. (2023) focuses on forecasting production in unconventional Bakken wells, comparing ten empirical production forecast models with advanced time series models like ARIMA, LSTM, and GRUs. The research reveals significant variability in the performance of empirical models across different wells, emphasizing the need for tailored approaches based on specific well characteristics. The ARIMA model, when fine-tuned, demonstrated superior predictive capabilities for many wells, outperforming several empirical models. This

study highlights the importance of incorporating well-specific conditions, such as lateral length and hydraulic fracturing details, to enhance model accuracy. By leveraging the strengths of both empirical and time series models, the research advocates for a synergistic approach to improve production forecasts in unconventional reservoirs.

3. Flow Properties and Implementation of the Work

Table 1 outlines the properties as stated in the project description. It summarizes the relevant characteristics essential for conducting the analysis outlined in this study. These properties serve as the foundation for developing the production forecast and analyzing pressure dynamics along the gas well. Each parameter listed in the table plays a crucial role in shaping the behavior of the gas reservoir and the performance of the production system. Therefore, a thorough understanding of these properties is essential for accurate modeling and interpretation of the results.

Table 1. Well and reservoir properties used as an input for this study

Parameters	Value
Constant Tubing Head Pressure (psig)	2000
Wellhead temperature (°F)	150
Initial reservoir pressure (psig)	4613
Bottomhole Temperature (T, °F)	200
Gas Specific Gravity (γ_g)	0.71
IPR Coefficient (C)	0.01
IPR Coefficient (n)	0.8
Pay thickness (ft)	100
Reservoir top depth (ft)	10000
Tubing Diameter (in)	2.441
Tubing relative roughness	0.0006
Reservoir permeability (md)	0.1
Reservoir porosity	0.16

Several articles (Laalam et al., 2023; Dranchuk and Abu-Kassem, 1975; Alagoz, 2023) have been consulted to ascertain the fluid properties. The Z-factor calculation method proposed by Dranchuk and Abu-Kassem (1975) was employed for determining the Z-factor. This approach, widely acknowledged in the literature, offers a robust framework for estimating the compressibility factor of the gas. By incorporating established methodologies from reputable sources, the study ensures accuracy and reliability in characterizing the fluid properties essential for subsequent analysis. Additionally, leveraging well-established techniques enhances the reproducibility and comparability of the study's findings with existing research in the field.

$$z = 1 + c1(tpr) * pr + c2(tpr) * pr^2 - c3(tpr) * pr^5 + c4(tpr) \tag{1}$$

$$pr = 0,27 * \frac{P_{pr}}{z * T_{pr}} \tag{2}$$

$$P_{pr} = \frac{P}{P_{pc}} \text{ and } T_{pr} = \frac{T}{T_{pc}} \tag{3}$$

$$P_{pc} = -3.6 * \gamma^2 - 131 * \gamma + 756.8 \tag{4}$$

$$T_{pc} = -74 * \gamma^2 + 349.5 * \gamma + 169.2 \tag{5}$$

$$c1(tpr) = A_1 + \frac{A_2}{T_{pr}} + \frac{A_3}{T_{pr}^3} + \frac{A_4}{T_{pr}^4} + \frac{A_5}{T_{pr}^5} \tag{6}$$

$$c2(tpr) = A_6 + \frac{A_7}{T_{pr}} + \frac{A_8}{T_{pr}^2} \tag{7}$$

$$c3(tpr) = A_9 * \left(\frac{A_7}{T_{pr}} + \frac{A_8}{T_{pr}^2} \right) \tag{8}$$

$$c4(tpr) = A_{10} * (1 + A_{11} * pr^2) * \frac{pr^2}{T_{pr}^3} * \exp(-A_{11} * pr^2) \tag{9}$$

where, P: psia and T: absolute temperature, °R. Ppc, Tpc, and Pr are dimensionless and A₁-A₁₁ are constant values for this z-factor calculation model which is also given in Table 2.

Table 2. Constant values for Z-factor calculation

Contents	Value
A1	0.3265
A2	-1.07
A3	-0.5339
A4	0.01569
A5	-0.05165
A6	0.5475
A7	-0.7361
A8	0.1844
A9	0.1056
A10	0.6134
A11	0.721

Viscosity calculations were conducted referencing the work of Lee et al. (1965), as presented in their paper titled "The Viscosity of Natural Gases" (Lee et al., 1965), published by the Society of Petroleum Engineers (SPE) under Paper 1340-PA. This seminal work provides valuable insights into the viscosity properties of natural gases, offering a foundational framework for our analysis. By integrating findings from this authoritative source, our study ensures comprehensive coverage of viscosity dynamics, contributing to a thorough understanding of fluid behavior within the gas well. Moreover, this reference serves as a cornerstone for validating and contextualizing our viscosity calculations within the broader literature landscape, thus reinforcing the credibility and robustness of our findings.

$$K = \frac{(9.4 + 0.02M_w)T^{1.5}}{209 + 19M_w + T} \tag{10}$$

$$X = 3.5 + \frac{986}{T} 0.01M_w \tag{11}$$

$$Y = 2.4 - 0.2X \tag{12}$$

$$\mu = K * \exp(X * \rho^Y) \tag{13}$$

unit analysis; T: absolute temperature, °R, μ : viscosity, micropoise and ρ : density, g/cc.

For density calculations,

$$\rho(lbm/cuft) = 2.7 * \frac{\gamma * P(psi)}{Z * T(^{\circ}R)} \tag{14}$$

Unit conversion between these two-density calculations,

$$1 \frac{lb_m}{cuft} = 0.0160185 \frac{g}{cc} \tag{15}$$

Gas formation volume factors and cumulative gas production rate were calculated with following equations,

$$Bg_i(rcf/scf) = 0.02827 \frac{ZT(^{\circ}R)}{P(psi)} \tag{16}$$

$$\Delta t = \frac{\Delta G_p(t)}{q_{avg}(t)} \tag{17}$$

$$G_p = G_i \left(1 - \frac{P_{avg}/Z}{P_i/Z_i} \right) \tag{18}$$

$$\Delta G_p = G_t \left(1 - \frac{P_{avg}_{t+\Delta t}/Z_{t+\Delta t}}{P_{avg}_t/Z_t} \right) \tag{19}$$

A linear temperature distribution was assumed, with the temperature gradient calculated from the bottom to the top of the well. The average temperature was employed for pressure drop calculations. This approach enables a simplified yet effective estimation of temperature variations along the wellbore, facilitating accurate assessments of pressure dynamics. By considering the average temperature, the analysis captures the overall thermal effects on pressure drop, thereby enhancing the comprehensiveness of the study. This methodology aligns with industry-standard practices for temperature modeling in gas well analyses, ensuring consistency and reliability in our findings. Additionally, by integrating temperature considerations into pressure drop calculations, our study provides a more holistic understanding of the factors influencing pressure behavior in the wellbore.

4. Solution Approach

Various models sourced from diverse literature were employed for the calculations, all executed using Microsoft Excel. Specifically, for the initial inquiry, the Fetkovich (1973), "The Isochronal Testing of Oil Wells" SPE Paper 4529, was referenced to construct the Inflow Performance Relationship (IPR) curves. Furthermore, Vertical Lift Performance (VLP) was derived from the problem statement, stipulating a constant bottom hole pressure (Pwf). Integrating these models offers a comprehensive framework for analyzing well performance under varying conditions, ensuring a robust and nuanced assessment of production dynamics. Additionally, by leveraging established methodologies from reputable sources, the study enhances the reliability and accuracy of its calculations, thereby bolstering the validity of its findings within the broader research landscape (Alagoz et al., 2023; Alagoz and Dundar, 2024).

To be able to construct the IPR curves, calculation of average reservoir pressure is required. The following equations were used for determining average reservoir pressure. Transient flow regime Darcy flow pressure square solution,

$$P_i^2 - P_{WF}^2 = \frac{711qZ_{avg}T\mu_{avg}}{hk} \left\{ \ln \left(\frac{4 \cdot 0.000264kt}{\gamma \cdot \phi(\mu c)r_w^2} \right) + 2s \right\} \quad (20)$$

Pseudo Steady State Darcy flow quadratic pressure square solution

$$P_{avg}^2 - P_{WF}^2 = \frac{1422qZ_{avg}T\mu_{avg}}{hk} \left\{ \ln \left(\frac{0.472r_e}{r_w} \right) + s \right\} \quad (21)$$

The starting point in this average reservoir calculation is flow rate for both flow regimes are identical at the onset of pseudo steady state. Using these equations firstly average reservoir pressure was calculated and then with other fluid properties, IPR curves were constructed with VLP curve. Next step, using the average production rate and readings from IPR vs VLP plot, production decline curve was plotted versus time. For the second question, Reynolds number and friction factor and it require variables were calculated and starting from the bottom of the well pressure losses calculated for each 100-ft interval up to 7,000-ft. Then small change in the velocity was recognized and from this point, pressure drop calculated for each 500-ft interval.

The friction factor was calculated using Chen's equation. First, Reynolds number was calculated using the following equation:

$$Re = \frac{4M_w q_{gsc} P_{sc}}{\pi D \mu R T_{sc}} \quad (22)$$

Then Chen's equation for the friction factor, using relative roughness ($\epsilon = k/D$):

$$\frac{1}{\sqrt{f_f}} = -4 \log \left\{ \frac{\epsilon}{3.7065} - \frac{5.0452}{Re} \log \left[\frac{\epsilon^{1.1098}}{2.8257} + \left(\frac{7.149}{Re} \right)^{0.8981} \right] \right\} \quad (23)$$

and for pressure drop calculations,

$$\Delta P = \frac{\rho \Delta u^2}{2} \left(\frac{1}{144} \right) + \rho \frac{g}{g_c} \Delta z \left(\frac{1}{144} \right) + \frac{2\rho f_f u^2 L}{g_c D} \left(\frac{1}{144} \right) \quad (24)$$

where; g : 32.2 ft/sec², g_c : 32.2 lbm.ft/lbf-sec², ρ : lbm/ft³, Δz : ft, u : ft/sec, L : ft and ΔP : pressure, psi.

And for fracture model calculations, the equation below employed.

$$S_f + \ln \left(\frac{X_f}{r_w} \right) = \frac{1.65 - 0.328 \ln(F_{CD}) + 0.11 [\ln(F_{CD})]^2}{1 - 0.18 \ln(F_{CD}) + 0.06 [\ln(F_{CD})]^2 + 0.05 [\ln(F_{CD})]^3} \quad (25)$$

$$X_f = \frac{L}{2} \quad (26)$$

$$F_{CD} = \frac{k_f b_f}{k X_f} \quad (27)$$

5. Computational Algorithm and Unit Analysis

5.1. Average Reservoir Pressure Calculation

Transient flow regime darcy flow pressure square solution,

$$P_i^2 - P_{WF}^2 = \frac{711qZ_{avg}T\mu_{avg}}{hk} \left\{ \ln \left(\frac{4 \cdot 0.000264kt}{\gamma \cdot \phi(\mu c)r_w^2} \right) + 2s \right\} \quad (28)$$

Pseudo Steady State darcy flow quadratic pressure square solution

$$P_{avg}^2 - P_{WF}^2 = \frac{1422qZ_{avg}T\mu_{avg}}{hk} \left\{ \ln \left(\frac{0.472r_e}{r_w} \right) + s \right\} \quad (29)$$

$$q = \frac{(P_i^2 - P_{WF}^2)hk}{711Z_{avg}T\mu_{avg} \left\{ \ln \left(\frac{4 \cdot 0.000264kt}{\gamma \cdot \phi(\mu c)r_w^2} \right) + 2s \right\}} \quad (30)$$

$$= \frac{hk(P_{avg}^2 - P_{WF}^2)}{1422Z_{avg}T\mu_{avg} \left\{ \ln \left(\frac{0.472r_e}{r_w} \right) + s \right\}}$$

$$t_{pss} = \frac{\phi(\mu c)A}{0.000264k} t_{DA} \quad (31)$$

Assumption and drainage are 40 acres, perfectly cylindrical reservoir, Darcy flow without skin ($t_{DA}=0.1$, $s=0$, $r_e=745$ ft, $r_w=0.328$ ft).

$$q = \frac{(P_i^2 - P_{WF}^2)hk}{711 \left\{ \ln \left(\frac{4 \cdot 0.000264k \cdot \frac{\phi(\mu c)A}{0.000264k} t_{DA}}{\phi(\mu c)r_w^2} \right) \right\}} \quad (32)$$

$$= \frac{hk(P_{avg}^2 - P_{WF}^2)}{1422 \left\{ \ln \left(\frac{0.472r_e}{r_w} \right) \right\}}$$

$$q = \frac{(P_i^2 - P_{WF}^2)hk}{711 \left\{ \ln \left(\frac{4 \cdot A t_{DA}}{\gamma r_w^2} \right) \right\}} = \frac{hk(P_{avg}^2 - P_{WF}^2)}{1422 \left\{ \ln \left(\frac{0.472r_e}{r_w} \right) \right\}} \quad (33)$$

$$A=40\text{acre} \cdot 43,560 \text{ ft}^2/\text{acre} = 1,742,400 \text{ ft}^2$$

$$\frac{(4613^2 - 1500^2)}{711 \left\{ \ln \left(\frac{4 \cdot 1742400(0.1)}{0.71 \cdot 0.328^2} \right) \right\}} = \frac{(P_{avg}^2 - 1500^2)}{1422 \left\{ \ln \left(\frac{0.472(745)}{0.328} \right) \right\}} \quad (34)$$

$$P_{avg} = 4338 \text{ psi} \quad (35)$$

5.2. Pressure Drop Unit Analysis

$$\Delta P = \frac{\rho \Delta u^2}{2} \left(\frac{1}{144} \right) + \rho \frac{g}{g_c} \Delta z \left(\frac{1}{144} \right) + \frac{2\rho f_f u^2 L}{g_c D} \left(\frac{1}{144} \right) \quad (36)$$

$$\Delta P - \text{kinetic energy} = \frac{\rho \Delta u^2}{2} \left(\frac{1}{144} \right) \quad (37)$$

$$= \frac{\text{lbm}}{\text{ft}^3} \left(\frac{\text{ft}}{\text{sec}} \right)^2 \frac{\text{lbf} \cdot \text{sec}^2}{\text{lbm} \cdot \text{ft}} = \frac{\text{lbf}}{\text{in}^2} = \text{psi}$$

$$\Delta P - \text{gravitational} = \rho \frac{g}{g_c} \Delta z \left(\frac{1}{144} \right) \quad (38)$$

$$= \frac{\text{lbm}}{\text{ft}^3} \frac{\text{ft}}{\text{sec}^2} \frac{\text{lbf} \cdot \text{sec}^2}{\text{lbm} \cdot \text{ft}} \text{ft} = \frac{\text{lbf}}{\text{in}^2} = \text{psi}$$

$$\Delta P - \text{friction} = \frac{2\rho f_j u^2 L}{g_c D} \left(\frac{1}{144} \right) \tag{39}$$

$$= \frac{\text{lbm lb f sec}^2 \text{ ft} \left(\frac{\text{ft}}{\text{sec}} \right)^2}{\text{ft}^3 \text{ lbm} \cdot \text{ft} \text{ ft} \left(\frac{\text{ft}}{\text{sec}} \right)} = \frac{\text{lb f}}{\text{in}^2} = \text{psi}$$

5.3. Reynolds Number Unit Analysis

$$Re = \frac{4M_w q_{gsc} P_{sc}}{\pi D \mu R T_{sc}} \tag{40}$$

$$= \frac{(4)(\text{lb}/\text{lb-mole}) \left(\text{ft}^3/\text{sec} \right) (14.7)(\text{psi})}{\pi(\text{in})(\text{cp})(10.731573) \left(\frac{\text{ft}^3 \text{ psi}}{R \text{ lb-mole}} \right) (520)(^\circ R)}$$

$$Re = \frac{(4)(\text{lb}/\text{sec})(14.7)}{\pi(\text{in})(\text{cp})(10.731573)(520)} \tag{41}$$

1cp = 0.001 Pa.sec

$$Re = \frac{(4)(\text{lb}/\text{sec})(14.7)}{\pi(\text{in})(0.001 \text{ Pa} \cdot \text{sec})(10.731573)(520)} \tag{42}$$

1Pa = 1N/m² (1N = kg.m/s²) 1Pa = kg/(m.s²)

$$Re = \frac{(4)(\text{lb}/\text{sec})(14.7)}{\pi(\text{in})(0.001 (\text{kg}/(\text{m} \cdot \text{s}^2)) \cdot \text{sec})(10.731573)(520)} \tag{43}$$

$$Re = \frac{(4)(\text{lb})(14.7)(\text{m})}{\pi(\text{in})(0.001 \text{ kg})(10.731573)(520)} * \frac{39.37 \text{ in}}{1 \text{ m}} \tag{44}$$

= dimensionless

But our unit constant= 132.0462708

To sum up,

$$Re = 132.0462708 \frac{M_w q_{gsc}}{D \mu} \tag{45}$$

D: diameter of tubing, in
 Mw: molecular weight of gas, lb/lb.mole
 q: gas flow rate, ft³/sec
 μ: gas viscosity, centipoise

5.4. Velocity Unit Analysis

$$u = \frac{4qzTP_{sc}}{\pi D^2 T_{sc} P} = \frac{(4)q \left(\frac{\text{ft}^3}{\text{s}} \right) zT(^\circ R) P_{sc}(14.7 \text{ psi})}{\pi D^2 (\text{in}^2) T_{sc}(520^\circ R) P(\text{psi}) \left(\frac{1}{144} \right)} = \text{ft/s} \tag{46}$$

$$u = 5.183 \frac{qzT}{D^2 P} \tag{47}$$

where; D: diameter of tubing, ft, q: gas flow rate, ft³/sec and T: absolute temperature, °R.

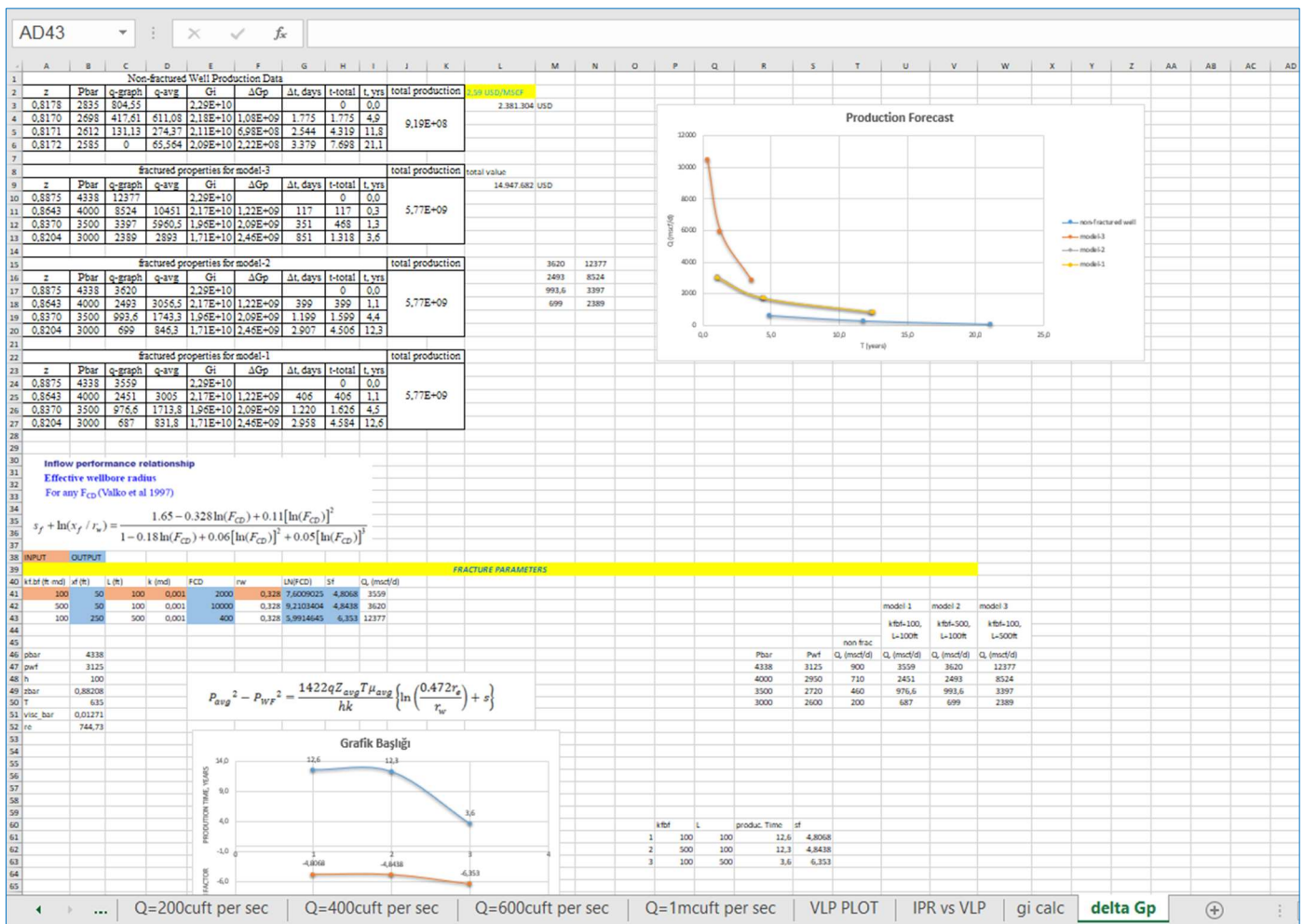


Fig. 1. A Snap of Microsoft Excel File

After these unit conversions, pressure losses calculated from 100-ft increment segments from bottom of the well, up to top of the well. For each increment, density, viscosity, velocity of gas and by using these parameters pressure losses and its components (friction, acceleration, and gravitational potential) were calculated. Each spreadsheet has its own function tabulated in Table 3 and an example of one application is in Fig. 1.

6. Output of the Work

The pressure distribution within the vertical gas well depicted in Fig. 2 plot reveals several notable components contributing to pressure drop. Notably, gravitational pressure losses emerge as the dominant factor influencing the pressure distribution along the wellbore. This observation underscores the significance of gravitational forces in dictating fluid behavior within the vertical well system under consideration. Additionally, the influence of kinetic energy change on pressure distribution is comparatively minimal, suggesting a minor impact

on overall pressure dynamics within the well. To provide further insight into the behavior of kinetic energy throughout the wellbore, an additional plot has been included in this report, offering a comprehensive understanding of pressure variations and their underlying mechanisms along the vertical gas well.

Table 3. Computational Algorithm of all excel spreadsheets

Name of the sheet	Properties
z factor	z factor calculations with ref-1
Q 0 cuft/sec	Pressure drop calculations for Q=0 cuft/sec
Q 5 cuft/sec	Pressure drop calculations for Q=5 cuft/sec
Q 69 cuft/sec	Pressure drop calculations for Q=69 cuft/sec
Q 200 cuft/sec	Pressure drop calculations for Q=200 cuft/sec
Q 400 cuft/sec	Pressure drop calculations for Q=400 cuft/sec
Q 600 cuft/sec	Pressure drop calculations for Q=600 cuft/sec
Q 1 mscft/sec	Pressure drop calculations for Q=1 mscft/sec
VLP PLOT	Vertical Lift Performance Plotting Calculations
IPR vs VLP	IPR and VLP Plotting Calculations
gi calc	initial gas in place calculation
delta Gp	production forecast, decline curve plot

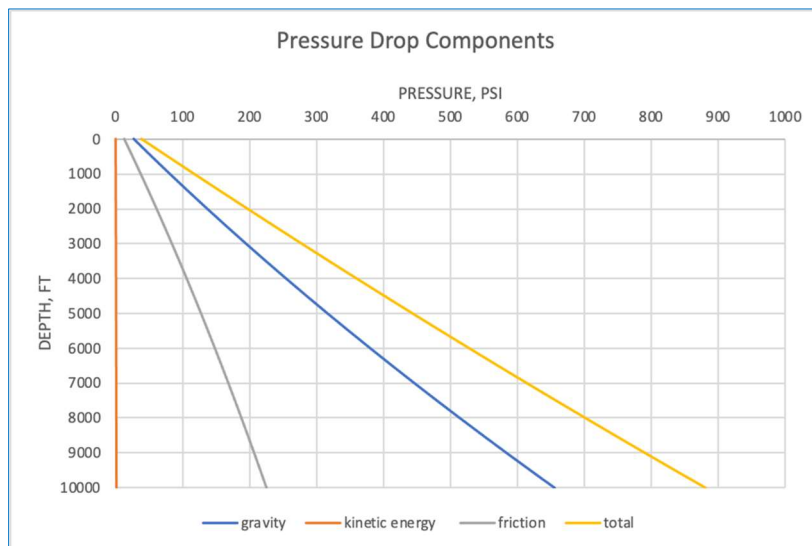


Fig. 2. Pressure Drop Along the Well

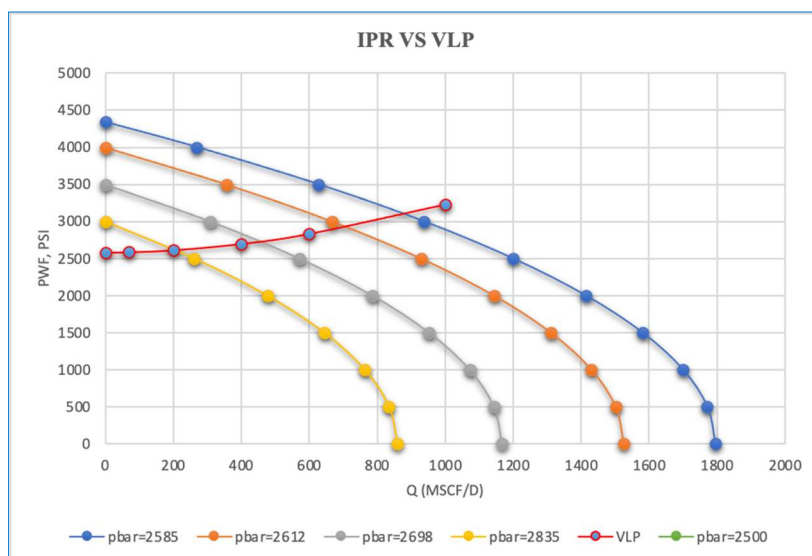


Fig. 3. IPR vs VLP Plot

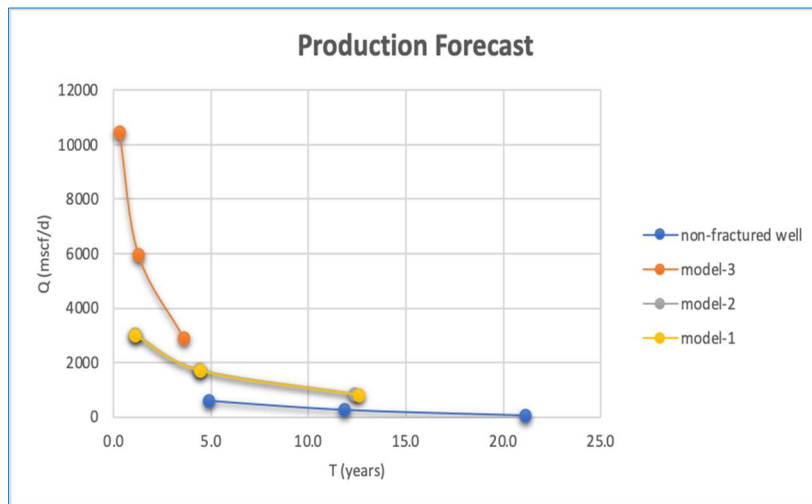


Fig. 4. Production Decline Curve

In conjunction with our findings, Figs. 2 and 3 offer visual representations of key aspects of our analysis. Fig. 3 depicts the Inflow Performance Relationship (IPR) versus Vertical Lift Performance (VLP) plot, providing a graphical illustration of the relationship between reservoir inflow and well performance.

Additionally, Fig. 4 shows cases the Production Decline Curve, offering insights into the expected decline in gas production over time.

Table 4 reveals a total gas production volume of approximately 919 million standard cubic feet (MMSCF), with the current market price of natural gas standing at \$2.03

USD per thousand standard cubic feet (MSCF). Based on these Fig. 4 the total value of the gas asset is estimated to be approximately \$1,866,000 USD. This valuation accounts for the cumulative revenue generated from the sale of gas over the production period, which spans 3.5 years.

By quantifying the economic value of the gas asset within the context of prevailing market conditions and production duration, stakeholders gain valuable insights into the financial implications and profitability of gas extraction operations. This analysis serves as a crucial decision-making tool for optimizing resource utilization, assessing investment returns, and formulating strategic plans to maximize revenue generation and profitability in the gas production sector.

Table 4. Non-fractured Well Production Data

z	Pbar	q-graph	q-avg	Gi	ΔGp	Δt, days	t-total	t, yrs
0,8178	2835	804,547		2,29E+10			0	0,0
0,8170	2698	417,607	611,077	2,18E+10	1,08E+09	1.775	1.775	4,9
0,8171	2612	131,127	274,367	2,11E+10	6,98E+08	2.544	4.319	11,8
0,8172	2585	0	65,5637	2,09E+10	2,22E+08	3.379	7.698	21,1

Table 5. Fractured Well Production Data (kfbf=100ft.md and L=500ft)

fractured properties for model-3								
z	Pbar	q-graph	q-avg	Gi	ΔGp	Δt, days	t-total	t, yrs
0,8875	4338	12377		2,29E+10			0	0,0
0,8643	4000	8524	10450,5	2,17E+10	1,22E+09	117	117	0,3
0,8370	3500	3397	5960,5	1,96E+10	2,09E+09	351	468	1,3
0,8204	3000	2389	2893	1,71E+10	2,46E+09	851	1.318	3,6

In Table 5, the case of fracture program model-3, the production forecast indicates a total gas yield of approximately 5.77 million million standard cubic feet (MMMSCF). Considering the current market price of natural gas at \$2.59 USD per thousand standard cubic feet (MSCF), the total value of the gas produced amounts to approximately \$11.72 million USD. This valuation accounts for the cumulative revenue generated from the sale of gas over the production period, which spans 3.6 years.

By quantifying the economic value of the gas extraction program within the context of prevailing market conditions and production duration, stakeholders can assess the financial viability and profitability of the fracture stimulation strategy. Such insights are instrumental in decision-making processes aimed at optimizing resource allocation, evaluating investment returns, and devising effective strategies to enhance revenue generation and overall project performance in the gas production industry.

Table 6 gives fracture program model-2 outputs, the projection indicates a collective gas output of approximately 5.77 million million standard cubic feet (MMMSCF). Given the prevailing market rate of natural gas, valued at \$2.03 USD per thousand standard cubic feet (MSCF), the total worth of the gas production stands at approximately \$11.72 million USD. This estimation encapsulates the sum of revenues generated from gas sales throughout the operational span, spanning a duration of 12.3 years.

By assessing the economic significance of the gas extraction initiative against current market dynamics and the extended production timeline, stakeholders can gauge the financial feasibility and profitability of the fracture stimulation strategy. Such insights serve as pivotal decision-making aids, guiding resource allocation, evaluating investment viability, and shaping strategic initiatives to optimize revenue generation and project performance within the gas production sector.

Table 6. Fractured Well Production Data (kfbf=500ft.md and L=100ft)

fractured properties for model-2								
z	Pbar	q-graph	q-avg	Gi	ΔGp	Δt, days	t-total	t, yrs
0,8875	4338	3620		2,29E+10			0	0,0
0,8643	4000	2493	3056,5	2,17E+10	1,22E+09	399	399	1,1
0,8370	3500	993,6	1743,3	1,96E+10	2,09E+09	1.199	1.599	4,4
0,8204	3000	699	846,3	1,71E+10	2,46E+09	2.907	4.506	12,3

Table 7. Fractured Well Production Data (kfbf=100ft.md and L=100ft)

fractured properties for model-1								
z	Pbar	q-graph	q-avg	Gi	ΔGp	Δt, days	t-total	t, yrs
0,8875	4338	3559		2,29E+10			0	0,0
0,8643	4000	2451	3005	2,17E+10	1,22E+09	406	406	1,1
0,8370	3500	976,6	1713,8	1,96E+10	2,09E+09	1.220	1.626	4,5
0,8204	3000	687	831,8	1,71E+10	2,46E+09	2.958	4.584	12,6

Table 7 reveals the fracture program model-1, our analysis projects a cumulative gas production of approximately 5.77 million million standard cubic feet (MMMSCF). At the prevailing market rate of \$2.03 USD per thousand standard cubic feet (MSCF) of natural gas, the total monetary value of this production stands at approximately \$11.71 million USD. This valuation encapsulates the collective revenue generated from gas sales over a duration of 12.6 years.

operations, emphasizing the importance of strategic decision-making in optimizing resource utilization and maximizing revenue generation. By elucidating the interplay between reservoir characteristics, operational parameters, and economic considerations, this study contributes to a deeper understanding of gas production dynamics and provides a valuable framework for guiding future research efforts and industry practices. Ultimately, the insights gleaned from this analysis are instrumental in informing stakeholders' decisions and driving advancements in gas production technologies and strategies.

By evaluating the economic significance of this gas extraction endeavor in light of current market conditions and the protracted production timeline, stakeholders can ascertain the financial viability and profitability of the fracture stimulation strategy. Such insights serve as pivotal decision-making tools, facilitating informed resource allocation, investment evaluation, and strategic planning to optimize revenue generation and project success within the gas production domain.

7. Conclusion

In conclusion, this paper has provided a comprehensive comparative analysis of gas production forecasts between non-fractured and fractured vertical gas wells. Through meticulous examination of factors such as Darcy flow, zero skin factor assumptions, and the influence of fracture stimulation techniques, valuable insights have been garnered into the dynamics of gas extraction efficiency and productivity. The findings underscore the significance of fracture stimulation in enhancing gas recovery rates and overall profitability, as evidenced by the substantial differences in production volumes and monetary values observed across various fracture program models. Moreover, the economic evaluations conducted highlight the substantial financial implications associated with gas production

References

Alagoz, E., 2023. Development and Analysis of a Program for Phase-Equilibrium Calculations Using the Peng-Robinson Equation of State. *International Journal of Earth Sciences Knowledge and Applications* 5 (1), 51-61. <http://www.ijeska.com/index.php/ijeska/article/view/276/292>.

Alagoz, E., Dundar, E.C., 2024. Forecasting Gas Well Production and Analyzing Pressure Dynamics. *Journal of Energy and Environmental Science* 2 (1), 000115. <https://doi.org/10.23880/jeesc-16000115>.

Alagoz, E., Giozza, G.G., 2023. Calculation of Bottomhole Pressure in Two-Phase Wells Using Beggs and Brill Method: Sensitivity Analysis. *International Journal of Earth Sciences Knowledge and Applications* 5 (3) 333-337. <http://www.ijeska.com/index.php/ijeska/article/view/324/323>.

Alagoz, E, Guo, Y., Li, L., 2023. Optimization of Fracture Treatment Design in a Vertical Well. *Petroleum and Petrochemical Engineering Journal* 7 (4), 000371. <https://doi.org/10.23880/ppej-16000371>.

Alagoz, E., Mungen, A.E., Bensenouci, F., Dundar, E.C., 2023. Computational Tool for Wellbore Stability Analysis and Mud Weight Optimization v1.0. *International Journal of Current Research Science Engineering Technology* 7 (1), 1-5.

- Chen, X., 2021. Enhancing Gas Well Performance Through Optimized Completion Methods. SPE Reservoir Evaluation & Engineering 17 (1), 34-48.
- Dranchuk, P.M., Abu-Kassem J.H., 1975. Calculation of Z Factor Natural Gases Using Equations of State. The Journal of Canadian Petroleum Technology PETSOC-75-03-03. <https://doi.org/10.2118/75-03-03>.
- Dundar, E.C., Alhemdi, A., Gu, M., 2019. Impact of natural fracture-induced elastic anisotropy on completion and Frac design in different shale reservoirs. Proceedings of the 7th Unconventional Resources Technology Conference. <https://doi.org/10.15530/urtec-2019-893>.
- Fetkovich, M. J., 121973. The Isochronal Testing of Oil Wells”SPE Paper 4529.
- Jones, R., Wang, L., 2020. Pressure Drop Analysis in Gas Wells: Implications for Well Performance. SPE Production & Operations 15 (2), 78-92.
- Laalam, A., Khalifa, H., Ouadi, H., Benabid, M.K., Tomomewo, O.S., Al Krmagi, M., 2024. Evaluation of empirical correlations and time series models for the prediction and forecast of unconventional wells production in Wolfcamp A formation. Paper presented at the SPE/AAPG/SEG Unconventional Resources Technology Conference, Houston, Texas, USA. <https://doi.org/10.15530/urtec-2024-4043738>.
- Laalam, A., Tomomewo, O.S., Khalifa, H., Bouabdallah, N., Ouadi, H., Tran, T.H., Perdomo, M.E., 2023. Comparative analysis between empirical correlations and time series models for the prediction and forecasting of unconventional Bakken wells production. Paper presented at the Asia Pacific.
- Lee, A.L., Gonzalez, M.H., Eakin, B.E., 1965. The Viscosity of Natural Gases Journal of Petroleum Technol 18 (8), 997-1000. <https://doi.org/10.2118/1340-PA>.
- Lee, H., Smith, M., 2018. Impact of Well Design on Gas Production: A Case Study." Journal of Petroleum Science and Engineering 12 (4), 112-125.
- Smith, J., Johnson, K., Brown, A., 2019. Forecasting Techniques for Gas Well Production: A Review. Journal of Petroleum Engineering 24 (3), 45-61.